A new ab initio potential energy surface for the collisional excitation of N_2H^+ by H_2

Annie Spielfiedel, Maria Luisa Senent, Yulia Kalugina, Yohann Scribano, Christian Balança, François Lique', and Nicole Feautrier'

Citation: J. Chem. Phys. **143**, 024301 (2015); doi: 10.1063/1.4923440
View online: http://dx.doi.org/10.1063/1.4923440
View Table of Contents: http://aip.scitation.org/toc/jcp/143/2
Published by the American Institute of Physics

A new *ab initio* potential energy surface for the collisional excitation of N_2H^+ by H_2

Annie Spielfiedel,[1] Maria Luisa Senent,[2] Yulia Kalugina,[3,4] Yohann Scribano,[5] Christian Balança,[1] François Lique,[1,3,a)] and Nicole Feautrier[1,b)]
[1]*LERMA, Observatoire de Paris, Sorbonne Université, UPMC Univ Paris 06, CNRS-UMR 8112, F-92195 Meudon, France*
[2]*Departamento de Química y Física Teóricas, IEM-CSIC, Serrano 121, Madrid 28006, Spain*
[3]*LOMC—UMR 6294, CNRS-Université du Havre, 25 rue Philippe Lebon, BP 1123, 76063 Le Havre, France*
[4]*Tomsk State University, 36 Lenin Ave., Tomsk 634050, Russia*
[5]*LUPM—UMR 5299, CNRS-Université de Montpellier, Place Eugene Bataillon, 34095 Montpellier Cedex, France*

(Received 27 April 2015; accepted 23 June 2015; published online 8 July 2015)

We compute a new potential energy surface (PES) for the study of the inelastic collisions between N_2H^+ and H_2 molecules. A preliminary study of the reactivity of N_2H^+ with H_2 shows that neglecting reactive channels in collisional excitation studies is certainly valid at low temperatures. The four dimensional (4D) N_2H^+–H_2 PES is obtained from electronic structure calculations using the coupled cluster with single, double, and perturbative triple excitation level of theory. The atoms are described by the augmented correlation consistent triple zeta basis set. Both molecules were treated as rigid rotors. The potential energy surface exhibits a well depth of ≃2530 cm^{-1}. Considering this very deep well, it appears that converged scattering calculations that take into account the rotational structure of both N_2H^+ and H_2 should be very difficult to carry out. To overcome this difficulty, the "adiabatic-hindered-rotor" treatment, which allows para-$H_2(j = 0)$ to be treated as if it were spherical, was used in order to reduce the scattering calculations to a 2D problem. The validity of this approach is checked and we find that cross sections and rate coefficients computed from the adiabatic reduced surface are in very good agreement with the full 4D calculations. © *2015 AIP Publishing LLC.* [http://dx.doi.org/10.1063/1.4923440]

I. INTRODUCTION

Modelling of physical and chemical conditions in the interstellar clouds requires to model the emission of various molecular species (neutrals, ions, or radicals). Several molecules can be used to probe different physical conditions of the molecular clouds. However, dense molecular clouds, and especially prestellar cores, suffer from strong depletion of most of the usual tracers (CO, CS, SO, etc., e.g., Ref. 1) and it has been found that only a few species survive in the gas phase. Among them, nitrogen bearing molecules are the best known (NH_3, N_2H^+, or CN[2–5]).

N_2H^+ was one of the first molecular ions detected in the interstellar medium (ISM).[6] Most observations concern the $j = 1 \rightarrow 0$ line, whose hyperfine structure helps to discriminate between opacity effects and collisional excitation effects, and thus, to study the deeper regions of cold cores contrarily to other species with larger opacities. However, to fully use the capabilities of N_2H^+ as a tracer of dense cloud conditions, state-to-state collisional data are needed.[7]

In addition, along with CN and HCN molecules, N_2H^+ is also used to determine $^{14}N/^{15}N$ abundance ratio in the universe.[8] ^{15}N-fractionation can have strong implications for our understanding of the diversity observed in the various bodies of the solar system. In cold dark clouds, $^{14}N/^{15}N$ abundance ratio is presently poorly constraint and the ratio varies from 150 to 1000 depending on the molecules and on the astronomical sources.[8–10] An important source of inaccuracies comes from the uncertainties linked with the N_2H^+ rate coefficients.

As a consequence, the determination of rate coefficients for collisions between the N_2H^+ ($X^1\Sigma^+$) molecule and the most abundant interstellar species (He and H_2) has been one of the important goals of molecular astrophysics in the past decades. The first N_2H^+–He rate coefficients were provided by Green[11] in 1975. More recently, Daniel *et al.*[12,13] have computed a new N_2H^+–He potential energy surface (PES) from highly correlated *ab initio* calculations and derived the corresponding rotational excitation rate coefficients. These last results differ within a few percent up to 100% from the former calculations by Green.[11] Cross sections and rate coefficients between hyperfine levels were then obtained using a recoupling technique.[13] In the absence of data with the H_2 collisional partner, He rate coefficients are generally used as a model for the H_2 ones.[14,15]

However, the necessity to compute exact H_2 rate coefficients and not using He ones as an estimate, particularly when the target is an ion, has been pointed out.[7] It is then crucial to provide the astronomical community with reliable N_2H^+–H_2 rate coefficients. Compared to the case of collisions with rare gas atoms, the increasing difficulty to consider H_2 as

a)Electronic address: francois.lique@univ-lehavre.fr
b)Electronic address: nicole.feautrier@obspm.fr

collider lies not only in the higher dimensionality of the system but also in the possibility for the interacting species to form chemical bonds and react. Indeed, during the collisions between N_2H^+ and H_2 molecules, inelastic and reactive collisions can compete. Hence, one has to check first that the probability of reactive collisions is very low compared to inelastic collisions due to an activation barrier or due to a significant endothermicity.

In this paper, we report first a preliminary study of the reactive pathways in order to check the barrier heights and endothermicity for the $N_2H^+ + H_2$ reactive collisions. This is followed by highly correlated *ab initio* calculations of the N_2H^+–H_2 PES. Taking into account the huge well depth found for the N_2H^+–H_2 interaction as well as the small rotational constant of the N_2H^+ molecule, converged scattering calculations are anticipated to be very challenging from a CPU point of view. As a consequence, in the third part of the paper, the "adiabatic-hindered-rotor" (AHR) treatment which allows para-$H_2(j = 0)$, the main collisional partner in the cold ISM, to be treated as if it were spherical is explored in order to reduce the scattering calculations to a 2D problem.

This paper is organized as follows. In Sec. II, we explore the reactive path during $N_2H^+ + H_2$ collisions. Sec. III describes the *ab initio* calculations of the N_2H^+–H_2 PES and its analytical representation. In Sec. IV, we use the AHR method to separate the rotation of hydrogen from the other degrees of freedom. Section V is devoted to the validation of the reduced dimension approach. Conclusions are finally drawn in Section VI.

II. REACTIVITY STUDY

As mentioned in the Introduction, $N_2H^+ + H_2$ collisions can be either inelastic or reactive collisions. At low temperatures, it can be anticipated that the reaction to form $H_3^+ + N_2$ is inefficient. Otherwise, N_2H^+ would not be easily detected. However, it is crucial to determine the temperature range where the reaction is inhibited in order to determine the validity area of a collisional study considering only the collisional excitation processes.

Hence, calculations have been performed, using GAUSSIAN 09,[16] to determine the region where the N_2H^+ cation does not react with molecular hydrogen. Thus, we have explored two possible reactive channels,

$$N_2H^+ + H_2 \rightarrow H_3^+ + N_2 \quad (1)$$

$$H_2 + N_2H^+ \rightarrow H_2N_2H^+ + h\nu. \quad (2)$$

Reaction (2) corresponds to a radiative association reaction. Radiative association reactions may be efficient in the cold ISM.

The first process is clearly endothermic favoring the formation of N_2H^+ from H_3^+ and N_2 and not the destruction of N_2H^+ due to collisions with H_2. Based on the explicitly correlated spin-restricted coupled cluster method with single, double, and perturbative triple excitations and the augmented correlation-consistent triple zeta basis set (RCCSD(T)-F12/aug-cc-pVTZ),[17,18] the enthalpy is calculated to be $\Delta H \approx 6300\ cm^{-1}$. Reaction (1) is then expected not to proceed at low and intermediate collisional energies that are encountered in the ISM.

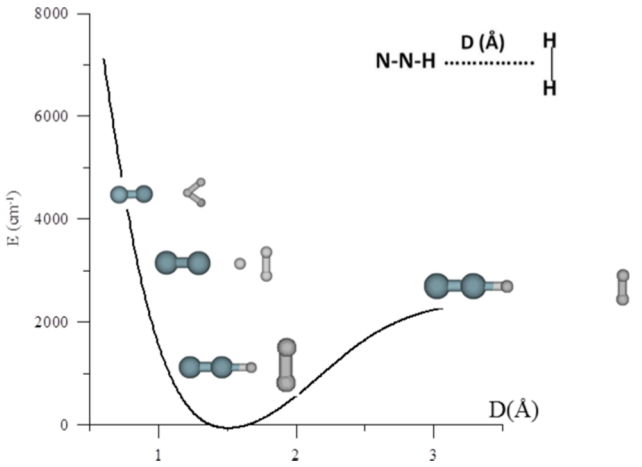

FIG. 1. The minimum energy pathway for the perpendicular attach. The minimum of the curve (E = 0.0 cm^{-1}) corresponds to D = 1.455 Å; NN = 1.0918 Å; NH = 1.0787 Å; HH = 0.7570 Å.

Using CCSD/aug-cc-pVTZ level of theory, the minimum energy pathways considering the H_2 molecule approaching perpendicular or parallel to the N_2H^+ principal axis have been computed. For this purpose, the total electronic energies have been calculated for different values of the D reaction coordinate (see Figs. 1 and 2). The remaining internal coordinates of the complex have been optimized.

Figures 1 and 2 display the one-dimensional potential energy curves. In Fig. 1, the D independent coordinate has been defined as the distance between the center of mass of the H_2 molecule and the hydrogen atom of N_2H^+. In Fig. 2, D represents the distance between the N_2H^+ hydrogen and one of the H atoms of the H_2 molecule. It can be inferred that the formation of N_2H^+ from $H_3^+ + N_2$ is not restricted by any barrier.

The second process is studied following the same procedure as described above, the minimum energy pathway being determined at the second-order Møller Plesset perturbation (MP2/aug-cc-pVTZ) level of theory. The formation of

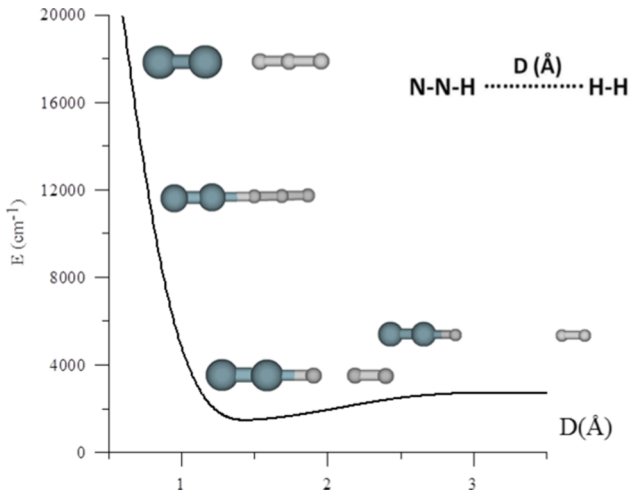

FIG. 2. The minimum energy pathway for the perpendicular attach. The minimum of the curve (E = 2038 cm^{-1}) corresponds to D = 1.6048 Å; NN = 1.0914 Å; NH = 1.0446 Å; HH = 0.7447 Å.

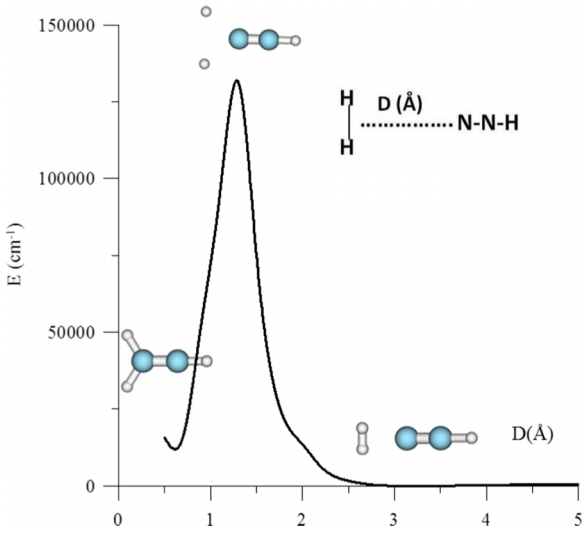

FIG. 3. The minimum energy path for reaction 2.

a $H_2N_2H^+$ complex is also endothermic (see Fig. 3). With the MP2/aug-cc-pVTZ, the enthalpy has been calculated to be $\Delta H \approx 14\,800$ cm^{-1}. In addition, a high potential barrier prevents the process. The barrier corresponds to the breaking of the H_2 molecule bond.

This study confirms that the formation of the diazenium ion ($N_2H_3^+$) is strongly endothermic as already noticed in Ref. 19 and that neglecting reactive channels for the study of collisional excitation of N_2H^+ by H_2 is valid at the typical temperatures of the ISM.

III. *AB INITIO* CALCULATIONS

Once it has been determined that inelastic collisions can be safely studied without considering the reactive pathways, we compute a PES for the rotational excitation of N_2H^+ by H_2.

A. *Ab initio* calculations of the PES

At typical interstellar temperatures, (T ≤ 300 K), molecules like N_2H^+ are generally in their ground vibrational state. The lowest vibrational bending frequency of N_2H^+ is ν_2 = 627.7 cm^{-1}.[20] The probability of vibrational excitation is very low and can be neglected in the scattering calculations. As a first guess, the collision partners may thus be considered as rigid. However, according to the large well depth found in the N_2H^+–H_2 PES (see Figs. 1 and 2), vibrational couplings may not be negligible even at low collisional energies. In addition, further dynamics calculations may span a range of energies which pass the threshold of the ν_2 bending mode (627.7 cm^{-1}) so that the rigid rotor approximation may be questionable.

In a recent study of the HCN–He system,[21] it has been shown that accounting for the bending motion during the collision affects weakly rotational excitation of the molecule compared to the rigid-rotor case, even when excited bending mode is energetically accessible. Moreover, in another recent study[22] on the collisional excitation of OH^+ by H (also a reactive system with a large endothermicity), it has been found

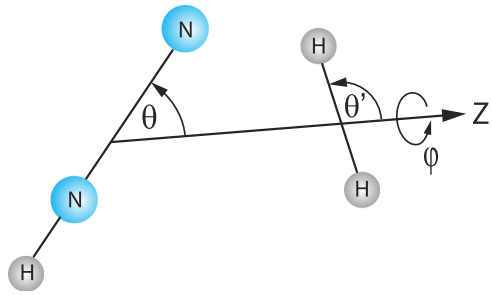

FIG. 4. The body-fixed Jacobi coordinates system for the N_2H^+-H_2 complex.

that exact close coupling calculations (including the reactive channels) were in good agreement with rigid rotor calculations. Hence, we believe that using a rigid rotor approach for studying the rotational excitation of N_2H^+ by H_2 will be accurate enough for astrophysical purpose as far as the temperatures remain low.

The N_2H^+ molecule in its ground electronic state has a linear equilibrium structure. The H_2 molecule was also considered as rigid. The body-fixed coordinate system used in the calculations is shown in Fig. 4. The geometry of the N_2H^+ and H_2 complex is characterized by three angles θ, θ', and φ and the distance R between the centers of masses of N_2H^+ and H_2. The polar angles of N_2H^+ and H_2 with respect to the z-axis that coincides with $\vec{R}$ are denoted, respectively, by θ and θ', while φ denotes the dihedral angle between half-planes containing the N_2H^+ and H_2 bonds. As shown previously,[23] a better description of the intermolecular potential is obtained by fixing the molecular distance at its average value in the ground vibrational level rather than at the equilibrium distance. Accordingly, we used a H_2 bond distance of r_{HH} = 1.448 a_0. Since such data are not available for N_2H^+, we chose internuclear distances fixed at their experimental equilibrium values:[24] r_{NN} = 2.065 a_0 and r_{NH} = 1.955 a_0.

Ab initio calculations of the four dimensional (4D) N_2H^+–H_2 PES were carried out at the coupled cluster with single, double, and perturbative triple excitation [CCSD(T)][25,26] level of theory using the MOLPRO 2010 package.[27]

Preliminary calculations have shown that an accurate description of both N_2H^+ and H_2 rotations has implied to compute the interaction potential for a large number of geometries. Then, the choice of the atomic basis set implies a compromise between accuracy and CPU time. We have performed interaction energy calculations for the N_2H^+–H_2 system with selected geometries using the aug-cc-pVXZ (X = T, Q,5) basis sets of Woon and Dunning.[28] Figure 5 presents a comparison of the performance of the various basis sets.

As can be seen, differences exist between results obtained using aVTZ, aVQZ, and aV5Z basis sets, the difference being around 5%-10% in the well area. However, as found previously,[29] inelastic rate coefficients (contrary to scattering resonances) are not highly sensitive to the potential well depth. Hence, we decide to limit the size of the basis set to aVTZ to maintain reasonable CPU time considering that the accuracy of the corresponding rate coefficients will be enough for astrophysical purpose. Note that the agreement between results obtained with the three basis sets increases with increasing radial coordinate R and that the accuracy of the PES obtained

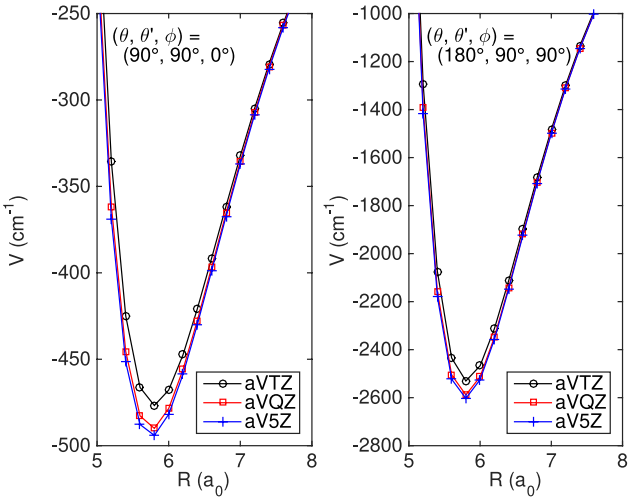

FIG. 5. Comparison of the performance of various basis sets in the calculation of the interaction energy of the N_2H^+–H_2 complex, for a few combinations of angular parameters (θ,θ',ϕ).

using the aVTZ basis set is very good in the long range as it will be also demonstrated below.

The radial scattering coordinate R was assigned 48 values from 4.0 a_0 to 40 a_0, the θ grid ranged from 0° to 180° in steps of 15°, whereas θ' and φ ranged from 0° to 180° and 0° to 90°, respectively, in steps of 30°. The geometry with $\theta = 0°$ and $\theta' = 0°$ corresponds to H–N–$N^+\cdots$H–H geometry.

In all calculations, the basis set superposition error (BSSE) was corrected at all geometries with the Boys and Bernardi[30] counterpoise correction scheme,

$$V(R,\theta,\theta',\varphi) = E_{N_2H^+-H_2}(R,\theta,\theta',\varphi) - E_{N_2H^+}(R,\theta,\theta',\varphi) - E_{H_2}(R,\theta,\theta',\varphi), \quad (3)$$

where the energies of N_2H^+ and H_2 subsystems are computed with the full basis set.

The R-dependence of the N_2H^+ and H_2 interaction energy for $\theta = 0°$, 90°, 180° is displayed in Fig. 6 for several (θ', φ) orientations. A very strong anisotropy as a function of the H_2 orientation is observed.

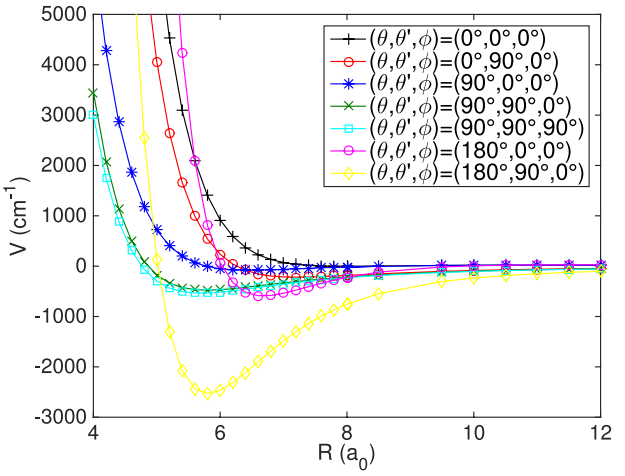

FIG. 6. Plot of the radial dependence of the CCSD(T) interaction energy for seven orientations. Energy is in cm^{-1}.

B. Analytical representation

In order to provide the potential for a wide range of intermolecular separations, we have performed analytical calculations of interaction energy on the basis of multipolar expansion. In the framework of the long-range approximation,[31] the interaction energy of the N_2H^+–H_2 system is a sum of the electrostatic (E_{elec}), induction (E_{ind}), and dispersion (E_{disp}) contributions. As the N_2H^+ molecule has a charge, we will limit the multipolar expansion to terms through the order of R^{-4} (we will neglect the dispersion interactions which vary as R^{-6}),

$$E_{elec} = \frac{1}{3}T_{\alpha\beta}\Theta^B_{\alpha\beta}q^A - \frac{1}{3}T_{\alpha\beta\gamma}\Theta^B_{\alpha\beta}\mu^A_\gamma. \quad (4)$$

$$E_{ind} = -\frac{1}{2}T_\alpha T_\beta \alpha^B_{\alpha\beta}(q^A)^2. \quad (5)$$

Superscripts A and B denote molecules N_2H^+ and H_2, accordingly. Tensor $T_{\alpha\beta\ldots} = \nabla_\alpha\nabla_\beta\ldots R^{-1}$ is the symmetric tensor relative to the permutation of any pair of subscripts. There is a summation over the repeated indexes.

The charge (q^A) of N_2H^+ molecule is equal to 1 a.u. The dipole (μ) and quadrupole (Θ) moments as well as static dipole polarizability (α) of monomers were calculated at the CCSD(T) level of theory with aVTZ basis set using the finite-field approach.[32] The quadrupole moment of hydrogen molecule is $\Theta_{zz} = 0.486$ a.u. (experimental value is 0.46 a.u.[33]) and the polarizability components are $\alpha_{xx} = \alpha_{yy} = 4.76$ and $\alpha_{zz} = 6.73$ a.u. Our average value of $\alpha = 1/3(2\alpha_{xx} + \alpha_{zz}) = 5.42$ a.u. agrees with experimental $\alpha = 5.42$ a.u.[34] The dipole moment of N_2H^+ molecule was calculated to be $\mu_z = -1.33$ a.u. which is in excellent agreement with the value -1.34 ± 0.20 from Ref. 35. The sign of dipole moment corresponds to the alignment of the molecule along z-axis with H atom pointing to the negative direction. It should be noted that all properties in Eqs. (4) and (5) are represented in the coordinate system of a complex, i.e., the above presented molecular properties should be appropriately rotated for any particular geometry.

In Fig. 7, we present the contributions to the interaction energy in long-range approximation for the equilibrium configuration of the N_2H^+–H_2 complex. The potential is dominated by electrostatic interactions. The leading electrostatic term is proportional to $\Theta^B q^A R^{-3}$ (see, Eq. (4)). There is a good agreement between the *ab initio* results and analytical representation for $R > 15$ a_0; thus, we can use the long-range approximation for generating additional data (R larger than 40 a_0) with confidence. The data obtained using Eqs. (4) and (5) were, then, incorporated into the fitting procedure.

It is most convenient to expand, at each value of R, the interaction potential $V(R,\theta,\theta',\varphi)$ in coupled spherical harmonics. For the interaction energy of two linear rigid rotors, we have used the expansion of Green,[36]

$$V(R,\theta,\theta',\varphi) = \sum_{l_1=0}^{16}\sum_{l_2=0}^{6}\sum_{l=|l_1-l_2|}^{l_1+l_2} v_{l_1l_2l}(R)A_{l_1l_2l}(\theta,\theta',\varphi), \quad (6)$$

where $v_{l_1l_2l}(R)$ are the radial functions and the basis functions $A_{l_1l_2l}(\theta,\theta',\varphi)$ are products of associated Legendre polynomials P_{lm},

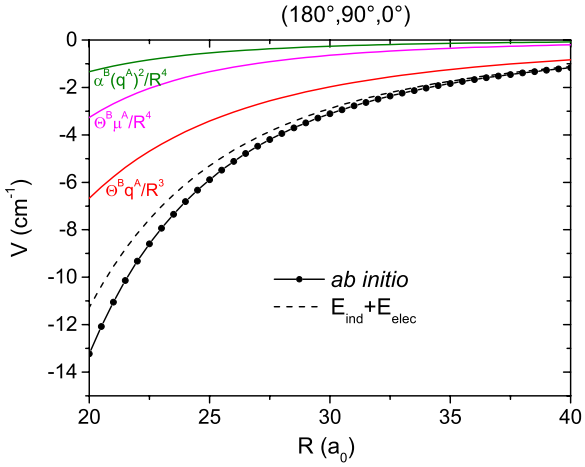

FIG. 7. Different contributions to the interaction energy of the N_2H^+–H_2 system for equilibrium configuration. Energy is in cm^{-1}. Solid black line — CCSD(T)/aug-cc-pVTZ calculations; dashed black line — total interaction energy in long-range approximation; solid color lines — contributions to interaction energy from Eqs. (4) and (5).

$$A_{l_1l_2l}(\theta,\theta',\varphi) = \sqrt{\frac{2l_1+1}{4\pi}}\{\langle l_1 0 l_2 0 \mid l_1 l_2 l 0\rangle P_{l_1 0}(\theta) P_{l_2 0}(\theta') + 2\sum_m (-1)^m \langle l_1 m l_2 - m \mid l_1 l_2 l 0\rangle \times P_{l_1 m}(\theta) P_{l_2 m}(\theta')\cos(m\varphi)\}, \quad (7)$$

where $\langle \ldots . | \ldots . \rangle$ is a Clebsch-Gordan coefficient. Here, indexes l_1, l_2 are associated with the rotational motion of N_2H^+ and H_2, accordingly, with the index l_2 being even due to the homonuclear symmetry of hydrogen molecule.

At each intermolecular separation R, the *ab initio* points were fitted to expression (6) using the least squares method. Such expansion gives in total 238 radial expansion coefficients $v_{l_1l_2l}(R)$. Due to complicated R-dependence of the coefficients $v_{l_1l_2l}(R)$, they were represented using cubic splines. The final fitted potential reproduces the long-range part with an average relative error less than 10^{-2}, the region of potential well -10^{-1}, and the repulsive wall ~1. We carefully checked that for $R \geq 40$ bohrs, there are only few nonzero coefficients and they have a smooth dependence with respect to R.

In order to evaluate the accuracy of our analytical representation, we computed the interaction potential for randomly selected geometries. In Fig. 8, we computed the deviations between *ab initio* values and analytical representation for these new values. As one can see, the agreement between the two sets of data is very good, the differences are generally lower than 1% in the potential well and in the repulsive part. The differences can be a bit larger for potential values ≃0 cm^{-1}. However, these differences will not significantly influence the scattering calculations.

C. Features of the N_2H^+–H_2 PES

Figures 9–11 present some cuts of the PES.

The equilibrium structure was found for a T-shape configuration with the H atom of N_2H^+ pointing towards the centre of mass of H_2 ($\theta = 180°$, $\theta' = 90°$, and $\varphi = 0°$). The corresponding distance between the centres of mass is $R = 5.8\ a_0$ with

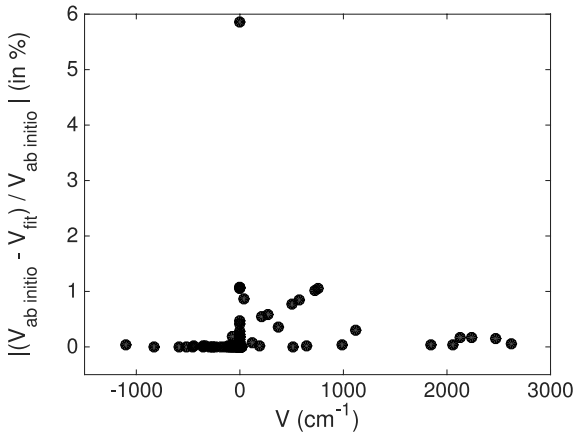

FIG. 8. Deviations (in %) between *ab initio* values and analytical representation for geometries randomly selected.

$\Delta E = -2531\ cm^{-1}$. Such geometry is in a good agreement with the one obtained by Bieske *et al.*[37] in their *ab initio* study of the N_2H^+–H_2 complex. Indeed, these authors found that the complex has a T-shaped minimum energy geometry with an N_2H^+–H_2 intermolecular bond length of ≃2.7 bohrs. Such bond length compares relatively well with the present bond length of ≃2.9 bohrs. Bieske *et al.*[37] also optimized the r_{NH} distance in their calculations that explain part of the difference we observe. Their value for the dissociation energy (≃2000 cm^{-1}) cannot be directly compared with the present one since their value is corrected from zero-point energy. However, the two values are in reasonable agreement.

The well depth is far greater than the ones usually found for interstellar molecules interacting with H_2, even for the isoelectronic anionic HCO^+-H_2 and CN^-–H_2 systems that present a well depth of approximately 1500 cm^{-1} [38] and 1000 cm^{-1},[39] respectively.

From Fig. 11 that shows the anisotropy of the interaction potential with respect to the N_2H^+ and H_2 rotations, we observe a relatively strong anisotropy of the PES with respect to the two θ and θ' Jacobi angles. Therefore, we may expect that rotational state of H_2 may influence the magnitude of the N_2H^+ excitation cross sections.

Taking into account the large well depth, we also anticipate the need to use very large rotational basis sets for both

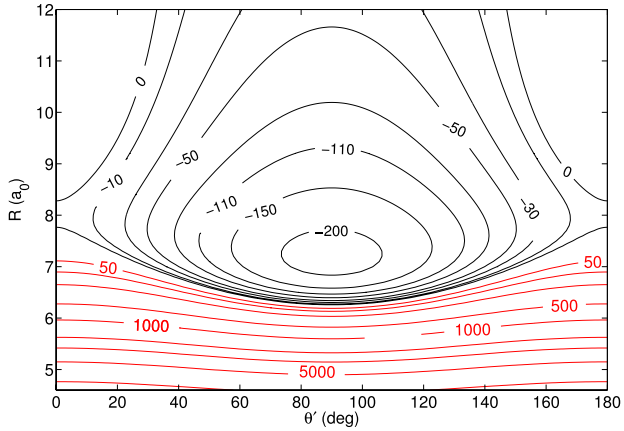

FIG. 9. Contour plot of the cut of the 4D PES for fixed $\theta = 0°$ and $\varphi = 0°$. Energy is in cm^{-1}. Red contour lines represent repulsive interaction energies.

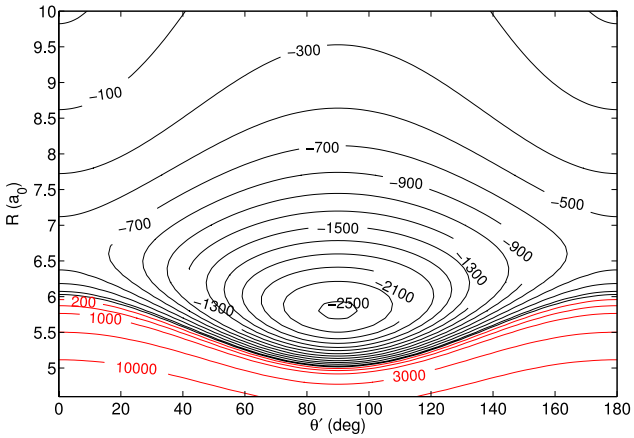

FIG. 10. Contour plot of the cut of the 4D PES for fixed $\theta = 180°$ and $\varphi = 0°$. Energy is in cm^{-1}.

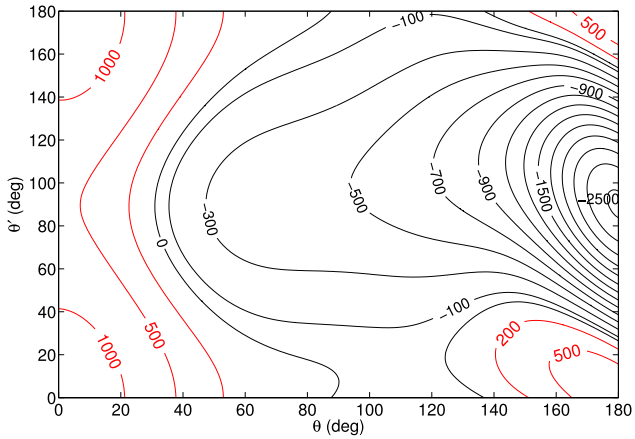

FIG. 11. Contour plot of the cut of the 4D PES for fixed $\varphi = 0°$ and $R = 5.8\ a_0$. Energy is in cm^{-1}.

N_2H^+ and H_2 to obtain full converged cross sections, even at low energies. For this reason, the AHR approach that reduces the 4D to a 2D problem will be explored below.

IV. REDUCED DIMENSIONAL POTENTIAL ENERGY SURFACES FOR COLLISIONAL EXCITATION STUDIES

Even using rigid rotor approximation, the study of the collisional excitation of N_2H^+ by H_2 remains very challenging from the dynamical calculations point of view. Taking into account the huge well depth as well as the small rotational constant of the N_2H^+ molecule, converged scattering calculations require to include at least 28 and 6 levels in the rotational basis for N_2H^+ and H_2, respectively. Scattering calculations with such a large number of channels would be prohibitive in terms of memory and CPU time. In addition, the large well depth also implies that converged collisional cross sections will have to be obtained by summing the partial cross sections over a very large number of total angular momentum even at low collisional energies.

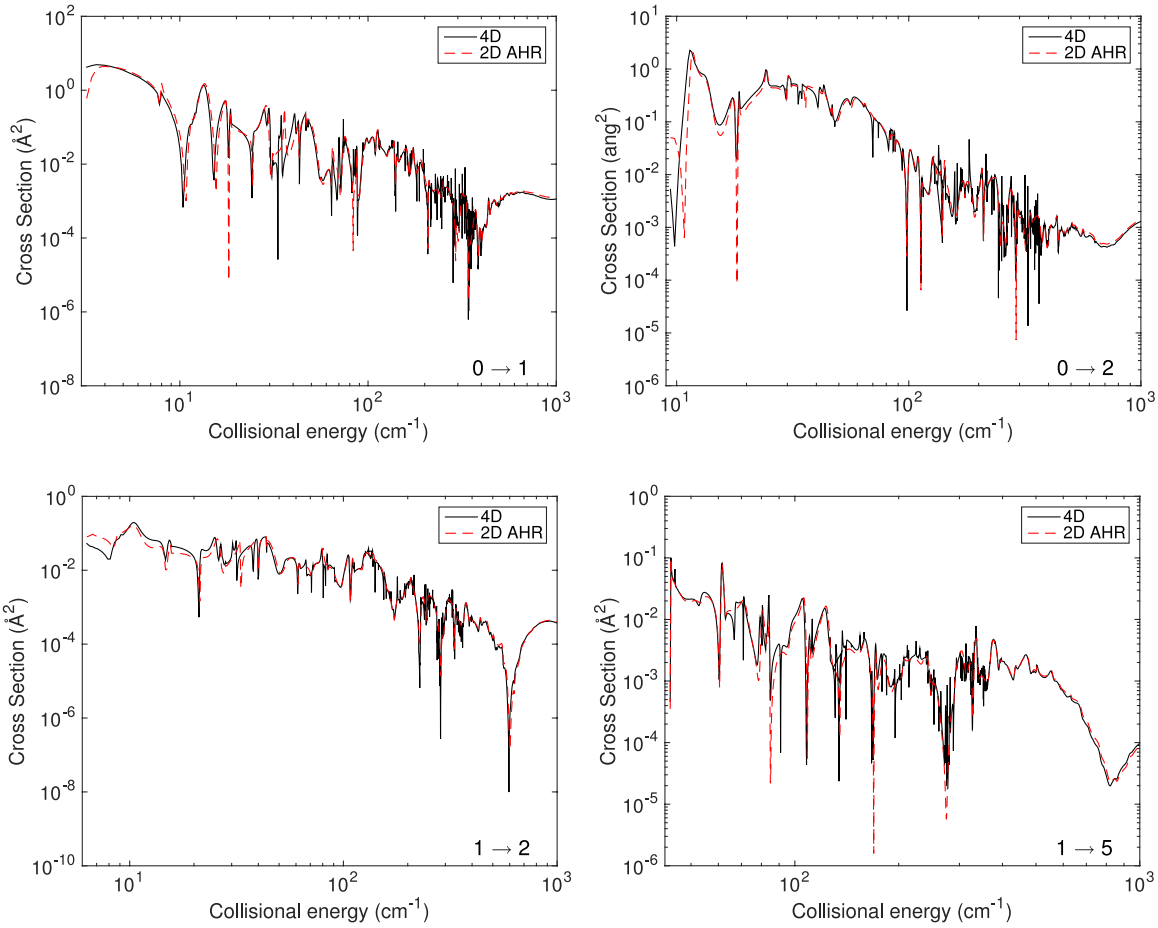

FIG. 12. Comparison of the $j = 0 \rightarrow j' = 1$, $j = 0 \rightarrow j' = 2$, $j = 1 \rightarrow j' = 2$, and $j = 1 \rightarrow j' = 5$ cross sections (for total angular momentum $J = 0$) for the N_2H^+–H_2 molecule in collision with para-H_2 as a function of the collision energy obtained from the full 4D PES (black lines) and the 2D AHR PES (red line).

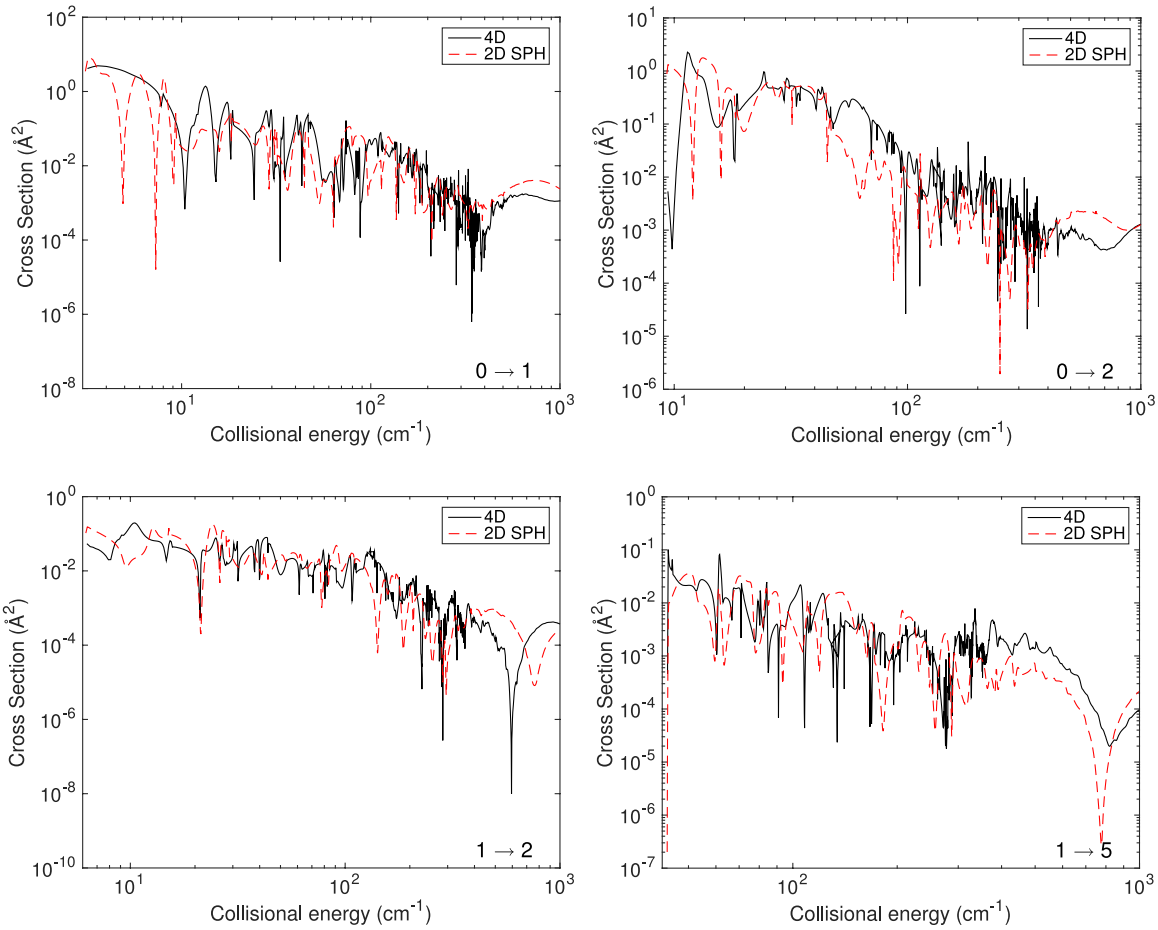

FIG. 13. Same as Fig. 12 for cross sections obtained from the full 4D PES (black lines) and the 2D SPH PES (red line).

It therefore seems reasonable to apply the "adiabatic-hindered-rotor" approach proposed by Hui Li *et al.*[40] and used successfully by Zeng *et al.*[41] for bound state calculations of H_2O-para-H_2 and by Scribano *et al.*[42] for the rotational excitation study of H_2O by collision with para-H_2.

This so-called AHR approximation consists of a Born-Oppenheimer type separation of the fast rotational motion of H_2 from the slower motions associated with the other intermolecular degrees of freedom. Then, the N_2H^+–H_2 4D-PES is reduced to a 2D-PES adapted to rotational excitation of N_2H^+ by para-$H_2(j = 0)$. For comparison, we have also considered a 2D-PES obtained by a simple-spherical average of the 4D-PES over H_2 orientations.[14]

We briefly summarize below the principle of this reduction dimensional scheme for N_2H^+–para-$H_2(j = 0)$. In the Born Oppenheimer (or quasi-adiabatic scheme), the four coordinates $(R, \theta, \theta', \varphi)$ are separated out into "fast" rotational coordinates of hydrogen $\mathbf{q} = \{\theta', \varphi\}$ and the "slow" other intermolecular coordinates $\mathbf{Q} = \{R, \theta\}$. This separation is governed by the high difference values of the rotational constants of the ion and of the hydrogen. Thus, following a similar approach used in electronic structure calculations, we compute at each grid point of the intermolecular coordinates $\mathbf{Q}_p$ a two dimensional eigenvalue $\mathcal{E}_n(\mathbf{Q}_p)$ for the (θ', φ) coordinates of H_2,

$$\hat{H}_{H_2}\Phi_n(\mathbf{q};\mathbf{Q}_p) = \mathcal{E}_n(\mathbf{Q}_p)\Phi_n(\mathbf{q};\mathbf{Q}_p), \tag{8}$$

where $\hat{H}_{H_2}$ represents the Hamiltonian operator of hydrogen defined by its kinetic operator and by the 4D-intermolecular potential $V(\mathbf{q}, \mathbf{Q})$. The above equation defines the quasi-adiabatic (or Born Oppenheimer) potential $\mathcal{E}_n(\mathbf{Q}_p)$ and the quasi-adiabatic wave function $\Phi_n(\mathbf{q};\mathbf{Q}_p)$ of fast coordinates, which both depend parametrically on the slow coordinates $\mathbf{Q}$.

In our near-adiabatic approximation, coupling between different adiabatic states and non-adiabatic derivative coupling terms is neglected.

Furthermore, we only consider the quasi-adiabatic ground state $\Phi_0(\mathbf{q};\mathbf{Q})$ wave function in the expansion of the full wave function. This approximation allows us to simplify the Born Oppenheimer Hamiltonian $\hat{H}_{BO} = \langle\Phi_0|\hat{H}_{4D}|\Phi_0\rangle$, which is then given by

$$\hat{H}_{BO} = -\frac{\hbar^2}{2\mu}\frac{\partial^2}{\partial R^2} + \frac{\hbar^2\mathbf{L}^2}{2\mu R^2} + \hat{T}_{N_2H^+} + \mathcal{E}_0(R,\theta), \tag{9}$$

where μ is the reduced mass of N_2H^+–H_2. This Hamiltonian describes the N_2H^+ molecule interaction with a pseudo-atom, point-like X. Eq. (8) was solved with a FBR (Finite Basis Representation) method using a basis set of spherical harmonics $Y_{j_2}^{m_2}(\mathbf{q})$ for the angular motion of hydrogen. This two-dimensional calculation was performed at each point of the two-dimensional $\mathbf{Q}$ grid. This basis set was used to diagonalize the Hamiltonian of Eq. (8). The basis set was extended up to $j_2^{max} = 4$. For para-H_2, only the even-j_2 values need to be considered.

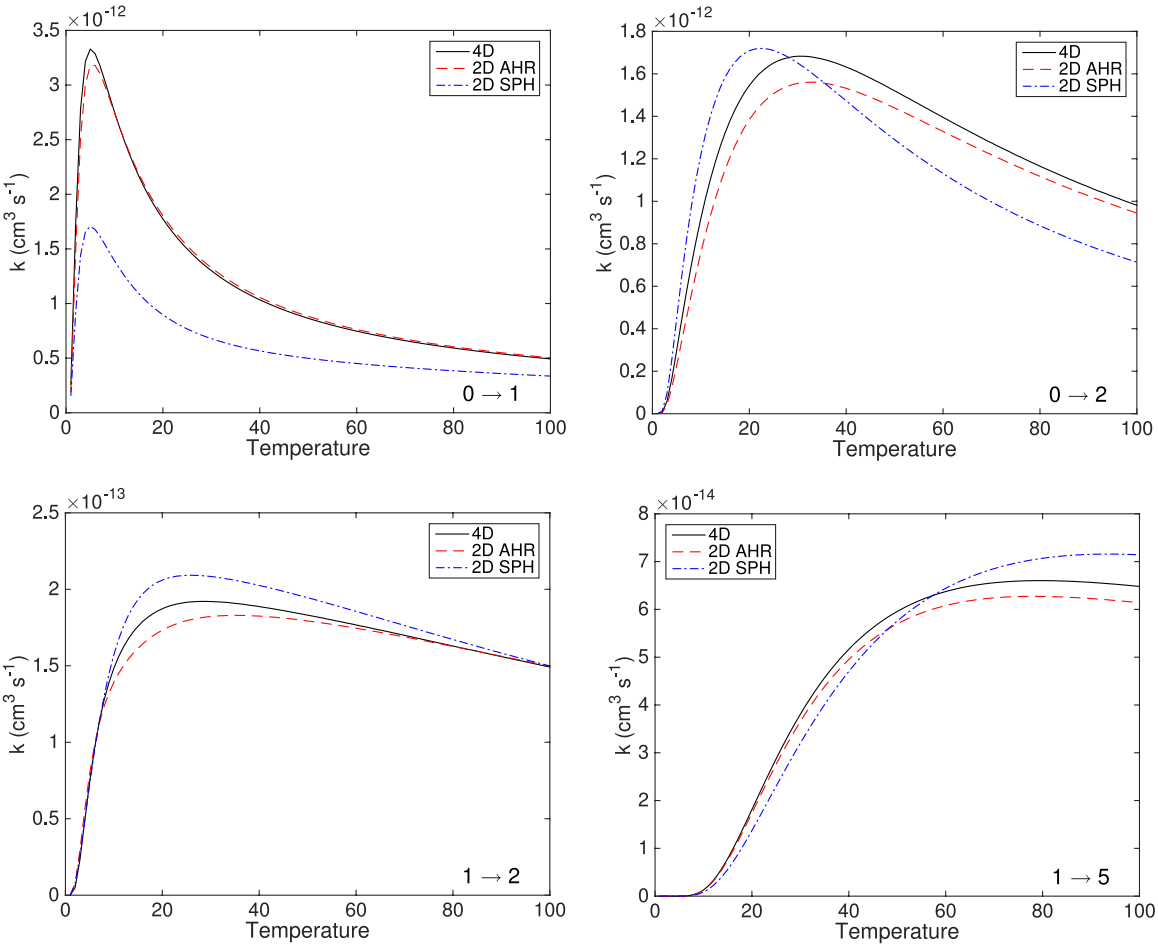

FIG. 14. Comparison of the $j = 0 \rightarrow j' = 1$, $j = 0 \rightarrow j' = 2$, $j = 1 \rightarrow j' = 2$, and $j = 1 \rightarrow j' = 5$ temperature-dependent rate coefficients obtained with the full 4D PES (solid black lines) and with the 2D AHR and the 2D SPH PESs (dashed red and dashed-dotted blue lines, respectively).

The adiabatic energies computed in this way at the **Q** grid points were then fitted to an analytical form adapted to close-coupling calculations. The adiabatic potential $V_{AHR}(R,\theta) = \mathcal{E}_0(R,\theta)$ was thus expanded as

$$V_{AHR}(R,\theta) = \sum_{\lambda} V_{\lambda}(R) P_{\lambda}(\cos\theta), \tag{10}$$

where $P_{\lambda}(\cos\theta)$ are the Legendre polynomials. The grid points (θ) describing the angular coordinate of the pseudo-atom X relative to N_2H^+ were chosen via a regular angular grid [0°–180°] for intermolecular distances R in the range 3–40 a_0.

At each intermolecular distance, the interaction potential $V_{AHR}(R,\theta)$ was then least-square fitted over a 19-term angular expansion following the procedure described by Werner *et al.*[43] The root-mean-square (rms) deviation between the analytical V_{AHR}-PES and the (averaged) *ab initio* data is 14 cm^{-1} for the full set of 1330 geometries and 0.5 cm^{-1} for the 1231 distances larger than 4.5 bohrs (when the highest part of the repulsive well is excluded).

The same fitting procedure was used to obtain the simple spherical-averaged PES (V_{SPH}) defined as

$$V_{SPH}(R,\theta) = \int_0^{2\pi} d\varphi \int_0^{\pi} d\theta' \sin\theta' V(R,\theta,\theta',\varphi). \tag{11}$$

The latter approach has been frequently used over the most recent years. Its accuracy strongly depends on the anisotropy of the PES with respect to the H_2 rotation.[14,44,45] For molecular ions like HCO^+ [38,46] or CN^-,[39] the approximation has been found to be relatively accurate, the agreement with exact calculations being better than 20%-30%.

Note that both the present AHR and spherical averaged (SPH) PES can only be used to describe the collisional excitation of N_2H^+ by para-$H_2(j = 0)$. Its use to describe collisional excitation by $H_2(j > 0)$ may lead to significant inaccuracies since $H_2(j = 0)$ and $H_2(j > 0)$ are generally different.[44,47–50]

V. VALIDITY OF REDUCED DIMENSIONAL APPROACHES

To ascertain the error introduced by the use of the reduced dimension PESs, we have compared the N_2H^+–para-H_2 partial cross sections obtained from 2D (both AHR and SPH) and 4D PESs at a fixed total angular momentum $J = 0$. Close-coupling calculations for the collisional excitation of N_2H^+ by para-$H_2(j = 0)$ were performed with the MOLSCAT code.[51] The N_2H^+ and H_2 energy levels were computed using the rotational constants of Sastry *et al.*[52] and of Huber and Herzberg,[53] respectively. In all these cases, to converge the calculations, the N_2H^+ rotational basis set includes all target states up to $j = 28$. Cross sections based on the full 4D PES include the coupling with the $j_2 = 2$, 4, and 6 levels of H_2.

The $j = 0 \rightarrow j' = 1$, $j = 0 \rightarrow j' = 2$, $j = 1 \rightarrow j' = 2$, and $j = 1 \rightarrow j' = 5$ cross sections, computed for a total angular momentum $J = 0$ with the above AHR and SPH PES, are compared to "exact" scattering calculations based on the 4D PES on Figs. 12 and 13. As it can be seen, the agreement between the full 4D and the AHR results is excellent, with differences of less than a few percents between those data. Similar conclusions are drawn for all the transitions. The only difference comes from the presence of some resonances in the calculations based on the 4D PES that are not present or well reproduced when using the 2D-AHR surface. However, those resonances influence only moderately the magnitude of the rate coefficients as shown in Fig. 14 for the same transitions.

From Fig. 13, we also observed that the 2D-SPH calculations ificantly differ from the exact calculations. The positions and magnitude of the resonances are very badly reproduced when using the SPH PES. Deviations also occur at high energies. Such differences are expected as found previously by Scribano *et al.*[42] for the rotational excitation study of H_2O by collision with para-$H_2(j = 0)$. As a consequence, the corresponding rate coefficients are in moderate agreement (20% up to a factor two, according to the transition and the temperature, see Fig. 14). However, it should be reminded that the rate coefficients have been computed from cross sections obtained from the only $J = 0$ partial wave and that converged SPH rate coefficients with respect to J may be in better agreement with exact calculations since the impact of the resonances will be moderate. Nevertheless, differences will probably remain owing to the differences seen at high energies.

As a conclusion, the adiabatic scheme is a real alternative to the full 4D treatment as it leads to much faster calculations and allows for the use of large rotational basis of the target. Unfortunately, this method is not presently available for collisions with ortho-H_2 where the Born-Oppenheimer approximation breaks down (work in progress).

Accurate description of collisional cross sections with para-H_2 cannot be obtained from H_2 treated as a sphere despite, as already observed for collisions between H_2 and an ion, the SPH approach allows to get the correct order of magnitude of the rate coefficients.

VI. CONCLUSION

This work presents a reliable 4-dimensional *ab initio* potential energy surface for the N_2H^+–H_2 system. Calculations were carried out at the CCSD(T) level with the aVTZ basis set of Woon and Dunning.[28] The global minimum occurs at 5.8 a_0 ($\theta = 180°$, $\theta' = 90°$, and $\varphi = 0°$) with a well depth of -2530.86 cm^{-1}. The interaction potential was then expanded in coupled spherical harmonics. A preliminary study of the reactive pathways shows that neglecting reactivity channels is valid for rotational excitation study at the typical temperatures of the ISM.

Considering the huge well depth as well as the small rotational structure of N_2H^+, it appears that fully converged scattering calculations that take into account both the rotational structures of the two molecules would be very challenging in terms of CPU time as well as in terms of required memory. Then, we have used the AHR approach proposed by Hui Li *et al.*[40] to obtain reduced-dimension potential energy surfaces. Within this scheme, the dynamics of collisions with para-$H_2(j = 0)$ is reduced from a 4D to a 2D problem. The comparison of cross sections and rate coefficients, computed for a total angular momentum $J = 0$, shows an excellent agreement between the 4D and the AHR results. This methodology will be used for the calculations of integral rotational excitation cross sections and rate coefficients by collisions with para-H_2.

Preliminary calculations at very low temperatures and including the hyperfine structure have been already obtained recently.[54] The new rate coefficients seem to increase the simulated line intensities obtained from radiative transfer calculations compared to the use of previous rate coefficients. It is then crucial to extend these calculations to higher temperature in order to interpret N_2H^+ observations in warmer regions. For collisional excitation with ortho-$H_2(j = 1)$ collisional partner that also has to be considered for astrophysical applications, approximate calculations using the present PES will also be performed in order to evaluate the differences between para-$H_2(j = 0)$ and ortho-$H_2(j = 1)$ rate coefficients. Depending on the magnitude of the differences, specific ortho-$H_2(j = 1)$ rate coefficients will then be computed. Approximate treatments (including the AHR treatment) will have to be explored in that case.

ACKNOWLEDGMENTS

This research was supported by the CNRS national program "Physique et Chimie du Milieu Interstellaire." F.L. and Y.K. also thank the Agence Nationale de la Recherche (ANR-HYDRIDES), contract No. ANR-12-BS05-0011-01. We acknowledge Laurent Pagani for stimulating this work.

[1]L. Pagani, J. R. pardo, A. J. Apponi, A. Bacmann, and S. Cabrit, Astron. Astrophys. **429**, 181 (2005).
[2]C. W. Lee, P. C. Myers, and M. Tafalla, Astrophys. J., Suppl. Ser. **136**, 703 (2001).
[3]M. Tafalla, P. C. Myers, P. Caselli, C. M. Walmsley, and C. Comito, Astrophys. J. **569**, 815 (2002).
[4]L. Pagani, A. Bacmann, S. Cabrit, and C. Vastel, Astron. Astrophys. **467**, 179 (2007); e-print arXiv:astro-ph/0701823.
[5]P. Hily-Blant, M. Walmsley, G. Pineau Des Forêts, and D. Flower, Astron. Astrophys. **480**, L5 (2008); e-print arXiv:0801.2876.
[6]E. Keto and P. Caselli, Astrophys. J. **201**, L25 (1975).
[7]E. Roueff and F. Lique, Chem. Rev. **113**, 8906 (2013).
[8]F. Daniel, M. Gérin, E. Roueff, J. Cernicharo, N. Marcelino, F. Lique, D. C. Lis, D. Teyssier, N. Biver, and D. Bockelée-Morvan, Astron. Astrophys. **560**, A3 (2013); e-print arXiv:1309.5782.
[9]L. Bizzocchi, P. Caselli, E. Leonardo, and L. Dore, Astron. Astrophys. **555**, A109 (2013); e-print arXiv:1306.0465.
[10]P. Hily-Blant, L. Bonal, A. Faure, and E. Quirico, Icarus **223**, 582 (2013); e-print arXiv:1302.6318.
[11]S. Green, Astrophys. J. **201**, 366 (1975).
[12]F. Daniel, M.-L. Dubernet, and M. Meuwly, J. Chem. Phys. **121**, 4540 (2004).
[13]F. Daniel, M.-L. Dubernet, M. Meuwly, J. Cernicharo, and L. Pagani, Mon. Not. R. Astron. Soc. **363**, 1083 (2005).
[14]F. Lique, R. Toboła, J. Kłos, N. Feautrier, A. Spielfiedel, L. F. M. Vincent, G. Chałasiński, and M. H. Alexander, Astron. Astrophys. **478**, 567 (2008).
[15]K. M. Walker, B. H. Yang, P. C. Stancil, N. Balakrishnan, and R. C. Forrey, Astrophys. J. **790**, 96 (2014).
[16]M. J. Frisch, G. W. Trucks, H. B. Schlegel, G. E. Scuseria, M. A. Robb, J. R. Cheeseman, G. Scalmani, V. Barone, B. Mennucci, G. A. Petersson *et al.*, GAUSSIAN 09, Revision D.01, Gaussian, Inc., Wallingford, CT, 2009.

[17]G. Knizia, T. B. Adler, and H.-J. Werner, J. Chem. Phys. **130**, 054104 (2009).
[18]T. H. Dunning, J. Chem. Phys. **90**, 1007 (1989).
[19]M. H. Matus, A. J. Arduengo, and D. A. Dixon, J. Phys. Chem. A **110**, 10116 (2006).
[20]G. K. Jarvis, Y. Song, C. Y. Ng, and E. R. Grant, J. Chem. Phys. **111**, 9568 (1999).
[21]O. Denis-Alpizar, T. Stoecklin, P. Halvick, and M. L. Dubernet, J. Chem. Phys. **139**, 034304 (2013).
[22]N. Bulut, F. Lique, and O. Roncero, "Exchange and inelastic $OH^+ + H$ collisions on the doublet and quartet electronic states," J. Phys. Chem. A (submitted).
[23]P. Jankowski and K. Szalewicz, J. Chem. Phys. **123**, 104301 (2005).
[24]J. C. Owrutsky, C. S. Guderman, C. C. Martner, L. M. Tack, N. H. Rosenbaum, and R. J. Saykally, J. Chem. Phys. **84**, 605 (1986).
[25]C. Hampel, K. A. Peterson, and H.-J. Werner, Chem. Phys. Lett. **190**, 1 (1992).
[26]J. D. Watts, J. Gauss, and R. J. Bartlett, J. Chem. Phys. **98**, 8718 (1993).
[27]H.-J. Werner, P. J. Knowles, G. Knizia, F. R. Manby, M. Schütz *et al.*, MOLPRO, version 2010.1, a package of *ab initio* programs, 2010, see http://www.molpro.net.
[28]D. E. Woon and T. H. Dunning, J. Chem. Phys. **100**, 2975 (1994).
[29]F. Lique, A. Spielfiedel, M. L. Dubernet, and N. Feautrier, J. Chem. Phys. **123**, 134316 (2005).
[30]S. F. Boys and F. Bernardi, Mol. Phys. **19**, 553 (1970).
[31]A. D. Buckingham, *Intermolecular Interactions: From Diatomics to Biopolymers* (Wiley, New York, 1978).
[32]H. D. Cohen and C. C. J. Roothaan, J. Chem. Phys. **43**, S34 (1965).
[33]A. D. Buckingham and J. E. Cordle, Mol. Phys. **28**, 1037 (1974).
[34]P. E. S. Wormer, H. Hettema, and A. J. Thakkar, J. Chem. Phys. **98**, 7140 (1993).
[35]S. Green, J. A. Montgomery, Jr., and P. Thaddeus, Astrophys. J. **193**, L89 (1974).
[36]S. Green, J. Chem. Phys. **62**, 2271 (1975).
[37]E. J. Bieske, S. A. Nizkorodov, F. R. Bennett, and J. P. Maier, Int. J. Mass Spectrom. Ion Processes **149**, 167 (1995).
[38]H. Massó and L. Wiesenfeld, J. Chem. Phys. **141**, 184301 (2014).
[39]J. Kłos and F. Lique, Mon. Not. R. Astron. Soc. **418**, 271 (2011).
[40]H. Li, P.-N. Roy, and R. L. Roy, J. Chem. Phys. **133**, 104305 (2010).
[41]T. Zeng, H. Li, R. J. Le Roy, and P.-N. Roy, J. Chem. Phys. **135**, 094304 (2011).
[42]Y. Scribano, A. Faure, and D. Lauvergnat, J. Chem. Phys. **136**, 5094109 (2012).
[43]H.-J. Werner, B. Follmeg, M. H. Alexander, and D. Lemoine, J. Chem. Phys. **91**, 5425 (1989).
[44]F. Dumouchel, J. Kłos, and F. Lique, Phys. Chem. Chem. Phys. **13**, 8204 (2011).
[45]Y. Kalugina, O. Denis Alpizar, T. Stoecklin, and F. Lique, Phys. Chem. Chem. Phys. **14**, 16458 (2012).
[46]O. Yazidi, D. Ben Abdallah, and F. Lique, Mon. Not. R. Astron. Soc. **441**, 664 (2014).
[47]M. Wernli, P. Valiron, A. Faure, L. Wiesenfeld, P. Jankowski, and K. Szalewicz, Astron. Astrophys. **446**, 367 (2006).
[48]G. Guillon and T. Stoecklin, Mon. Not. R. Astron. Soc. **420**, 579 (2012).
[49]Y. Kalugina, J. Kłos, and F. Lique, J. Chem. Phys. **139**, 074301 (2013).
[50]M. Lanza, Y. Kalugina, L. Wiesenfeld, and F. Lique, J. Chem. Phys. **140**, 064316 (2014).
[51]J. M. Hutson and S. Green, MOLSCAT computer code, version 14, distributed by Collaborative Computational Project No. 6 of the Engineering and Physical Sciences Research Council, UK, 1994.
[52]K. V. L. N. Sastry, P. Helminger, E. Herbst, and F. C. De Lucia, Chem. Phys. Lett. **84**, 286 (1981).
[53]K. P. Huber and G. Herzberg, *Molecular Spectra and Molecular Structure. IV. Constants of Diatomic Molecules* (Van Nostrand Reinhold, New York, 1979).
[54]F. Lique, F. Daniel, L. Pagani, and N. Feautrier, Mon. Not. R. Astron. Soc. **446**, 1245 (2015); e-print arXiv:1410.5669.